Wetland eco-engineering: measuring and modeling feedbacks of oxidation processes between plants and clay-rich material

Rémon Saaltink[1], Stefan C. Dekker[1], Jasper Griffioen[1,2], Martin J. Wassen[1]

[1] Department of Environmental Sciences, Copernicus Institute of Sustainable Development, Utrecht University, Utrecht 3508 TC, The Netherlands.

[2] TNO Geological Survey of the Netherlands, Princetonlaan 6, 3584 CB Utrecht, The Netherlands

Corresponding author

Rémon Saaltink

e-mail: r.m.saaltink@uu.nl

tel: +31 30 253 2404

Abstract

Interest is growing in using soft sediment as a foundation in eco-engineering projects. Wetland construction in the Dutch lake Markermeer is an example: here dredging some of the clay-rich lake-bed sediment and using it to construct wetland will soon begin. Natural processes will be utilized during and after construction to accelerate ecosystem development. Knowing that plants can eco-engineer their environment via positive or negative biogeochemical plant–soil feedbacks, we conducted a six-month greenhouse experiment to identify the key biogeochemical processes in the mud when *Phragmites australis* is used as an eco-engineering species. We applied inverse biogeochemical modeling to link observed changes in pore water composition to biogeochemical processes. Two months after transplantation we observed reduced plant growth and shriveling and yellowing of foliage. The N:P ratios of plant tissue were low and these were affected not by hampered uptake of N, but by enhanced uptake of P. Subsequent analyses revealed high Fe concentrations in the leaves and roots. Sulfate concentrations rose drastically in our experiment due to pyrite oxidation; as reduction of sulfate will decouple Fe-P in reducing conditions, we argue that plant-induced iron toxicity hampered plant growth, forming a negative feedback loop, while simultaneously there was a positive feedback loop, as iron toxicity promotes P mobilization as a result of reduced conditions through root death, thereby stimulating plant growth and regeneration. Given these two feedback mechanisms, we propose the use of Fe-tolerant species rather than species that thrive in N-limited conditions. The results presented in this study demonstrate the importance of studying the biogeochemical properties of the situated sediment and the feedback mechanisms between plant and soil prior to finalizing the design of the eco-engineering project.

Keywords: Drying; Fe-P; Iron toxicity; P mobilization; PHREEQC; Pyrite

1. Introduction

Nowadays, natural processes are being used across the world to achieve fast ecosystem development while at the same time providing opportunities for developing hydraulic infrastructure, a concept called Building with Nature (BwN) (Temmerman et al., 2013). Though mostly focused on water safety and coastal protection (e.g. Borsje et al., 2011), BwN can also be applied for the management of fine sediments. A relevant application could be to use soft sediments as material for building freshwater wetlands. Here, vegetation can be used as an eco-engineer (Jones et al., 1994), to modify the environment (Lambers et al., 2009). When fine sediments are used for the construction of wetlands, however, the use of eco-engineers is anticipated to pose challenges in relation to crest stability, consolidation and soil formation.

In the Netherlands, a soft, clay-rich lake-bed sediment is causing serious turbidity problems in the Markermeer (an artificial lake of 691 km^2): primary productivity is impeded and biodiversity in the lake is declining (Vijverberg et al., 2011; Noordhuis et al., 2014). Because the lake is shallow, wind-induced waves frequently induce high bed shear stress, which causes sediment to be resuspended (Vijverberg et al., 2011). To improve the ecological conditions in the lake, plans are underway to dredge some of the soft, clay-rich sediment and use it to construct approximately 10,000 ha of wetlands.

Plants produce root exudates which influence soil formation by enhancing microbiological activity (Holtkamp et al., 2011), biological weathering and nutrient cycling (Taylor et al., 2009; Bradford et al., 2013). An example is the ability of plant roots to mobilize P by ligand exchange and dissolution of Fe-bound P (Fe-P) by citrate and oxalate excretion (Gerke et al., 2000). Plant roots may also enhance consolidation processes in substrate by increasing horizontal and vertical drainage (O'Kelly, 2006).

However, both negative and positive plant–soil feedbacks exist, in which the physical and chemical properties of the soil affect plant development and vice versa (Ehrenfeld et al., 2005). Therefore, when looking at soil formation, it is important to study the signs and strengths of these plant–soil feedback mechanisms. For example, nutrient conditions co-determine the type of plant community that develops (e.g. Olde Venterink, 2011), which in turn influences the nutrient conditions in the soil itself (Onipchenko et al., 2001). As feedback mechanisms differ between plant species (Ehrenfeld et al., 2005), it is essential to determine which eco-engineer is most appropriate for accelerating ecosystem development in these sediments.

De Lucas Pardo (2014) found that the Markermeer mud deposits had a high water content (20–60% of fresh weight) and were largely anoxic, with oxygen present only in the top 2 mm. Therefore, when such mud is taken from the lake and spread out in contact with the air, biogeochemical plant–soil processes related to oxidation and drying of the top soil are expected to play a significant role. Two types of clay-rich deposits are the intended sediment for the wetland. Their composition is the product of a combination of historical and present-day factors. Prior to 1932, the year in which the dam cutting off the Zuiderzee from the North Sea was completed, this was a marine environment into which several rivers discharged, including a branch of the river Rhine (the river IJssel). Hence, a near-shore marine deposit underlies the present-day soft, clay-rich sediment. This soft, clay-rich layer is produced by bioturbation and physical weathering and continuously resuspends as a result of wave action (Van Kessel et al., 2008; De Lucas Pardo et al., 2013). This layer accumulated after 1976, when northward sediment transport was blocked by a second dam that separated Markermeer from IJsselmeer, thus allowing suspended matter to resettle on top of the marine deposit. We can therefore distinguish two layers: an upper disturbed mud layer prone to bioturbation and erosion, and a relatively undisturbed layer below.

We set up an experiment to monitor the chemical composition of pore water to identify the biogeochemical plant–soil feedback processes that occur when oxidation, drying and modification by plants alter the biogeochemical conditions of these two sediment types, thus in turn affecting vegetation development. Our study has two subsidiary aims: to ascertain how *Phragmites australis* eco-engineers its environment by expediting biogeochemical processes in the deposits, and to simulate the geochemical differences between disturbed mud and undisturbed clay deposits and relate these to the processes identified from the pore water by using PHREEQC for inverse modeling. In addition, we altered the grain size of the disturbed mud deposit by adding inert sand to see how grain size distribution impacts pore water chemistry.

Changes in biogeochemical processes that are related to oxidation are expected to play a major role as *P. australis* is known for its high radial oxygen loss (Brix et al., 1996; Dickopp et al., 2011; Smith and Luna, 2013). Oxidation of the sediment will decrease the concentration of phytotoxins typically found in waterlogged soils, such as iron, and therefore will have a positive effect on plant development. This will be more pronounced in undisturbed mud, which is largely anoxic, than in disturbed mud, of which the top layer is already oxidized and where bioturbation modified the sediment. The type of biogeochemical processes altered will depend on the intrinsic properties of the different sediment types, which will be examined in this study.

2. Material and Methods

2.1 Set-up

A greenhouse experiment was conducted for six months at the test facility of Utrecht University. A basin of 4 m^2 (2 x 2 m) was filled with artificial rainwater and was refreshed every two weeks. At regular intervals, the chemistry of the water was checked to ensure that the water composition remained stable during the experiment. The artificial rainwater was made by adding 15 µmol $NH_4(SO_4)$, 50 µmol $NaNO_3$ and 30 µmol NaCl to osmosis water. These values reflect the average rainwater composition in the Netherlands for the period 2012–2013 (LMRe, 2014).

The sediments used include the soft, clay-rich layer (Mud_{soft}) and the underlying, consolidated, Zuiderzee deposit (Clay). In principle, both sediments have the same origin and were collected in the same area. We also included a third sediment type (Mud_{sand}), as it is expected that Mud_{soft} will be too soft for constructing wetlands: a 1:1 mixture was made by mixing mud with Dorsilit® crystal silica sand (c. 99% SiO_2) which had been autoclaved for one hour at 120 °C prior to mixing. The sand grains of this material are 0.3-0.8 mm in diameter with D50 being 0.57 mm. The Mud_{soft} and Clay sediments were collected by mechanically dredging in the southern part of the lake and were stored in air-tight containers at 4 °C prior to the start of the experiment.

Plastic pots (diameter 10 cm, depth 18 cm) with a perforated base were filled to within 1 cm from the top with one of the three sediment types used (t = 0). In each pot, two soil moisture samplers (Rhizon Flex-5cm; Rhizosphere, Wageningen, the Netherlands) were installed horizontally at depths of 1 cm and 11 cm below the sediment surface (these depths are hereafter referred to as D_1 and D_{11}), its tip reaching 5 cm from the pot wall. The pots were stood in rows in the basin. The water level was maintained at 9 cm so that the sediment at D_{11} remained saturated while the sediment at D_1 could oxidize and dry. Each sediment type had 13 replicates.

Reed seedlings (*Phragmites australis*) had been grown in nutrient-poor peat and when 35–40 days old (experimental time t = 22 days), a single reed seedling was planted per pot in eight of the replicates, leaving five replicates unplanted. Any other seedlings that germinated spontaneously in the pots were removed immediately.

2.2 Chemical analysis

Soil moisture at D_1 and D_{11} was collected from the moisture samplers on days 0, 3, 10, 22, 36, 64, 92, 134 and 174 from five of the pots per condition. The samples from the five replicates were pooled and chemically analyzed. Chloride, NH_4, NO_2, NO_3 and SO_4 were determined using ion chromatography (IC); Ca, Fe, K, Mn, Na, P, Si and Sr were determined with Inductively Coupled Plasma Optical Emission Spectrometry (ICP-OES), pH by an ion-specific electrode, and alkalinity was measured by a classic titration method.

Sediment samples were collected for each sediment type at t = 0 and were freeze–dried and stored anoxically prior to geochemical analysis. The major elements were determined using ICP-OES following an aqua regia destruction. Total S content was measured on an elemental CS analyzer and the mineralogical composition was determined with X-ray diffraction (XRD). A sequential extraction method based on Ruttenberg (1992) was applied to characterize solid P speciation. The method involves five steps (Table 1), the first four of which were carried out anoxically. Loss on ignition (LOI) was determined by slowly heating to 1000 °C. LOI was also used as a proxy for organic matter content and total carbonates by calculating the weight loss between 105–550 °C for organic matter and the weight loss between 550–1000 °C for total carbonates (Howard, 1965). Cation exchange capacity (CEC) of the sediments was calculated from the organic matter content and the amounts and types of clay minerals present (Bauer and Velde, 2014).

Fifty seedlings of *P. australis* randomly chosen from the seedlings grown for the experiment were used to determine the initial tissue contents of Fe, K, P, and N. Their roots, shoots, and leaves were separated and air dried. The air–dried material was then ground and analyzed with total reflection X-ray fluorescence (TXRF) to determine tissue contents of Fe, K, and P. Nitrogen content was determined on an elemental CN analyzer. At the end of the experiment (t = 174), the plants in the pots were harvested and subjected to the same procedure, to determine the tissue contents of Fe, K, P, and N.

2.3 Modeling of biogeochemical processes

To identify important biogeochemical processes during the incubation experiments, we modeled with PHREEQC (Parkhurst and Apello, 2013). PHREEQC modeling is frequently used in geochemical research focusing on issues of water quality: examples include investigating mineral weathering in a mountain river (Lecomte et al., 2005), deducing geochemical processes in groundwater (Belkhiri et al., 2010) and investigating the interaction between two aquifers (Carucci et al., 2012). Here, we applied it to identify biogeochemical plant–soil processes during the oxidation and natural drying out of the soil.

The model approach is based on mass-balance equations of preselected mineral phases (reactants). The mineral phases can either precipitate (leave the solution) or dissolve (enter the solution) and these are expressed in mole transfers. As we only know the dynamics in concentrations of the pore water, we applied inverse modeling in which all possible combinations of the mass-balance equations are accepted within a range of measured pore water concentrations ± 4%. We can simulate infiltration or evaporation rates from the pore water. Since in freshwater mud deposits, the dissolution or precipitation of salts (e.g. NaCl) is negligible and can be ignored, the change in pore water Cl concentration was used to calculate the amount of water evaporated or infiltrated.

To enable the model to attribute some of the chemical changes to cation-exchange processes we included an assemblage of exchangers (X): CaX_2, FeX_2, KX, MgX_2, NaX and NH_4X. The sum of this assemblage was defined as CEC calculated from the sediment composition. CEC is important, since it can buffer some of the biogeochemical processes in sediments by adsorption or desorption of cations.

We identified three time frames in our models: 1) oxidation and natural drying out of the soil before the seedlings were transplanted into the pots (t = 0–22 days); 2) initial stage of plant growth (t = 22–64 days); and 3) the stage in which roots started to influence pore water chemistry (t = 64–176 days). These time frames were identified by analysing the chemical data that was collected. When concentrations at D11 in the planted condition started to deviate from the unplanted condition, this was seen as a sign that plant roots started to influence pore water chemistry.

Inverse modeling was applied for all combinations (sediment type, plant/no plant, and depth) for each time frame. For every combination, several valid simulations were found, due to small differences in the amount of mole transfers attributed to the mineral phases. Here we present the plausible simulation with the least amount of mole transfers for each combination.

2.4 Statistical analysis

Statistical analysis was carried out using the programs R and SPSS. Differences in sediment, pore water and plant tissue concentrations between sediment treatments were determined using one-way ANOVA with a Tukey's honestly significant difference (HSD) post hoc test. No statistics could be applied to the mineralogical sediment composition (XRD analysis) due to absence of replicates.

3. Results and Discussion

First, the three sediment types will be compared in terms of certain geochemical and mineralogical elements. Next, the composition of the pore water will be introduced and will be linked to biogeochemical processes by presenting and discussing the PHREEQC model simulations. Then, the plant response is presented and discussed in terms of biomass and plant tissue chemistry. Lastly, the implications for eco-engineering will be discussed.

3.1 A brief comparison between sediment types

Table 2 shows the geochemical composition of the disturbed Mud_{soft} and Mud_{sand} and undisturbed Clay sediments used in this study. The differences between Mud_{soft} and Mud_{sand} are solely attributable to the presence of inert Dorsilit®.

The total sediment concentrations of Al, Fe, Mg, Mn, Na, P, and Zn were significantly higher in Clay than in Mud_{soft} ($p < 0.05$). The quartz content was also higher in Clay, which suggests that there were more reactive minerals in this type of sediment.

Sequential P extraction revealed that the significant difference in total P consists of a significantly lower content of Fe-P in Mud_{soft} than in Clay (279 mg/kg versus 772 mg/kg; $p < 0.01$). The presence of Fe-P in the anoxic Clay sediment was unexpected, as in anoxic conditions Fe prefers to bind with S to form FeS_2. However, after exhaustion of S, precipitation of Fe(II) phosphates may occur (Jilbert and Slomp, 2013). Another possibility is that the reduction of crystalline Fe(III) is not complete in the anoxic sediment because kinetic processes are slow (Canavan et al., 2007). This is likely the case in Markermeer, given our strict anoxic procedures for storage and analysis of the samples. The exchangeable (or loosely sorbed) P was low in Mud_{soft} and Clay, indicating that only a small part of the total P found in the sediments was readily available for uptake. The other three P-pools were fairly similar and did not differ significantly between the two types of sediment ($p = 0.42$ for Ca-bound P; $p = 0.11$ for detrital P; and $p = 0.94$ for Organic P).

The mineralogical analysis (XRD) showed not only that the quartz content was lower in Mud_{soft} than in Clay (37% versus 48%) but that the amounts of calcite and pyrite did not differ between the two types of sediment (9% calcite and 0.6% pyrite). The amount of phyllosilicates (sum of illite, smectite, kaolinite, and chlorite) was higher in Mud_{soft} than in Clay: 43% versus 30%. This must also have caused the CEC to be higher in Mud_{soft}, as the organic matter content did not differ much between the two (7.2% in Mud_{soft} and 6.8% in Clay).

3.2 Pore water composition

Figure 1 presents time series for the pore water concentrations of the three macronutrients N, P, and K. The initial decrease in NH_4 and increase in NO_x at a depth D_1 for the planted conditions was most likely caused by nitrification as a result of oxidation (Figure 1a–f). At the end of the experiment, almost all dissolved inorganic nitrogen had been removed from the pore water in the pots with plants, whereas in the pots without plants, the NH_4 concentrations remained substantial. Furthermore, a high peak of NO_x was observed in Clay sediments at day 10 of the experiment. At a depth D_{11}, no large changes were found in general for NH_4 and NO_x.

A sharp decline in soluble P was visible at D_1 for all three sediments, probably because P precipitated with Fe(III) when oxygen penetrated the top layer (Figure 1g–i). However, in Clay this decline was preceded by an increase in P. After several weeks, a thin moss layer started to develop on top of the Mud_{soft} sediment, which probably prevented oxygen from penetrating and thereby increased the P concentrations (Figure 1g). Similar developments were observed for Mud_{sand} although here the moss layer developed much later. In Clay, no moss grew throughout the experiment.

Concentrations of K were higher than concentrations of N and P and increased in the first few weeks (Figure1j–l). No difference was found between pots at D_{11} with or without plants. However, K was significantly higher at D_1 in the planted pots with Mud_{sand} ($p < 0.05$).

Although it may be important to study measured concentrations of nutrients in pore water in order to understand plant functioning, deriving biogeochemical processes from measured data is problematic changes in pore water can be caused by multiple processes such as drying, dilution, dissolution, and precipitation. Figure 2 reveals that the drying of soils at D_1 was probably an important factor, because we observed an initial increase in Cl that indicated that Cl could not dissolve in the three sediments used (e.g. halite dissolution). Drying will have influenced other variables as well, such as sulfate (Figure 2d–f). Comparing the patterns of Cl and SO_4 suggests that the change in SO_4 concentrations at D_1 should be partly attributed to drying out of soils and partly either to dissolution (e.g. pyrite oxidation) or to precipitation (e.g. gypsum formation). This highlights the need to use geochemical reaction models like PHREEQC to inversely derive biogeochemical processes from measured data.

3.3 Pore water processes (PHREEQC model simulations)

The main pore water processes modeled by PHREEQC are presented in Table 3. For clarity, only major reactants are included in this Table. Supplementary Tables A1 and A2 present mole transfers for all reactants used, as well as the number of valid simulations per combination found.

3.3.1 Phase 1: Oxidation and drying (t = 0–22 days)

As discussed in section 3.2, initial drying of soils occurred at D_1 immediately after exposure to air. In the model, this is illustrated by high evaporation rates expressed as H_2O loss (2300–3400 mmol l^{-1} day^{-1}; Table 3). The model accounts for this loss by adjusting the solution fractions before calculating other mole transfers.

Exposure to air also leads to oxidation, more so at D_1 than at D_{11} (Table 3). The increase in measured sulfate is partly explained as pyrite oxidation (109–270 µmol l^{-1} day^{-1} for D_1 and 20.1–36.2 µmol l^{-1} day^{-1} for $D_{11,}$ respectively). Oxidation of pyrite also produces iron oxyhydroxides and protons which in turn promotes dissolution of calcite. The overall reactions are

$$FeS_2 + 3.75O_2 + 3.5H_2O \rightarrow Fe(OH)_3 + 2SO_4^{2-} + 4H^+ \quad (1)$$

followed by calcite dissolution

$$CaCO_3 + H^+ \rightarrow Ca^{2+} + HCO_3^- \quad (2)$$

The mole transfers for pyrite and calcite presented in Table 3 indicate that not enough calcite is dissolved to buffer all H^+ produced by dissolution of pyrite. Indeed, a drop in pH was observed at the beginning of the experiment (not shown). However, the mineralogical composition presented in Table 2 shows that the amount of calcite (9%; 900 mmol) far exceeds that of pyrite (0.6%; 50 mmol). These numbers suggest that even if all pyrite were to be oxidized, enough calcite is present to buffer all H^+ produced (200 mmol). Note that for Mud_{sand} these values are lower due to mixing with Dorsilit®.

Some aeration occurred at D_{11}. The O_2 fluxes ranged between 61 and 119 µmol l^{-1} day^{-1}, which resulted in small amounts of pyrite being oxidized (20–36 µmol l^{-1} day^{-1}). However, sulfate concentrations did not rise, as a result of subsequent precipitation with Ca to form gypsum (53–73 µmol l^{-1} day^{-1}). Furthermore, the cation-exchange-capacity (CEC) of the sediments buffered some processes in pore water chemistry by net adsorption of cations at D_1 and net desorption at D_{11}.

The processes described above occurred in all three sediments, although oxidation was higher in Mud_{soft} than in Mud_{sand} and Clay, probably because higher evaporation rates in Mud_{soft} enhanced oxidation and affected other reactants related to oxidation.

3.3.2 Phase 2: Initial stage of plant growth (t = 22–64 days)

While the pore water compositions did not show clear differences between unplanted and planted conditions during the initial stage of plant growth, the inverse modeling provided clear evidence for differences at D_1. However, chemical differences between unplanted and planted conditions for Mud_{sand} might simply be attributed to concentration/dilution due to H_2O loss/gain (-996 to 380 mmol l^{-1} day^{-1}).

Overall, more pyrite was oxidized in the planted conditions, though the rates are much lower than in the first phase (0–64.3 µmol l^{-1} day^{-1}). This observation provides evidence that plants may enhance pyrite oxidation by radial oxygen loss (i.e. root aeration). Ferric oxide production on pyrite surfaces probably impeded further oxidation of pyrite, which is a common phenomenon in carbonate-buffered conditions (Nicholson et al., 1990). Indeed, the total pyrite that had oxidized after 64 days (6.3 mmol for Mud_{soft}, 2.5 mmol for Mud_{sand} and 6.2 mmol for Clay, calculated from the rates presented in Table 3) corresponds to a small fraction of total pyrite present (50 mmol).

Saturation with gypsum led to precipitation of SO_4 and Ca at D_1. Table 3 shows that with the exception of Mud_{sand}, mole transfers were lower for planted conditions; the probable reason is that citric acid production by root tips retarded gypsum precipitation (Prisciandaro et al., 2005). This process was not relevant at D_{11}, as here aeration (and subsequent sulfate production) by plant roots was minor (in the case of Clay) or absent (in the case of Mud_{soft} and Mud_{sand}).

The thin moss layer that started to develop after several weeks in the unplanted condition on top of the Mud_{soft} sediment slowed down the aeration rate to 2.62 µmol l^{-1} day^{-1} and might be the reason for the moderate increase in P, which probably resulted from $Fe(OH)_3$ dissolution (0.95 µmol l^{-1} day^{-1}) (Figure 1g, Table 3).

3.3.3 Phase 3: Root influence (t = 64–176 days)

Phase 3 took place in the autumn, when temperatures were lower and therefore the soils did not dry out; hence there was a net gain in H_2O. The gain was less in planted conditions, due to uptake of water by roots.

The fully grown plants continued to influence pore water chemistry at D_1, but in the unplanted conditions the chemical changes were minor (Table 3). Radial oxygen loss continued the oxidation processes described in the previous sections. It should be noted that *P. australis* is known to have higher radial oxygen loss than other wetland species (Brix et al., 1996; Dickopp et al., 2011; Smith and Luna, 2013), so the aeration effect found in this study cannot be assumed to hold for other species.

In contrast to the previous phase, in phase 3 the influence of roots was clearly visible at D_{11} for all three sediments. All planted sediments showed increased aeration and subsequent oxidation of pyrite due to radial oxygen loss, with a notable difference between Mud_{soft} (lower) and Mud_{sand} (higher). This is somewhat surprising, as the belowground biomass was significantly higher in Mud_{soft} (section 3.4). It indicates that increasing the average grain size by adding sand enhanced aeration, even when root biomass production was low.

3.4 Plant response

Above- and belowground biomass were significantly higher in Mud_{soft} and Clay than in Mud_{sand} (Figure 3; $p < 0.02$). The difference between the two Mud sediments cannot be explained by nutrient concentrations in pore water or light conditions in the greenhouse, as these were the same for the two sediments. As biomass production in Mud_{sand} was not limited by chemical or biological properties relative to Mud_{soft}, it seems likely that the reason for the lower biomass production in Mud_{sand} is a difference in physical properties. Voorhees et al. (1975) and Bengough and Mullins

(1990) showed that so-called mechanical impedance (i.e. the resistance to penetration by the root tip) was higher in loamy sand than in clay, which was attributed to the higher bulk density of the loamy sand. Therefore, increasing the bulk density of Mud_{soft} by mixing with sand increased the mechanical impedance and this might explain the lower biomass production we observed in Mud_{sand}.

P. australis invested more in its root system than in its shoots and leaves for all sediments (Figure 3; $p < 0.01$). More investment in roots implies a limitation of N, P, and/or S (Ericsson, 1995; Shipley and Meziane, 2002). Figures 1a–i and 2d–f show that the N and P concentrations were indeed low in the planted conditions but that SO_4 was high, which rules out S limitation. During the experiment, we had observed reduced plant growth and shriveling and yellowing of foliage 2 months after transplantation, which might have been caused by nutrient limitation.

Figure 4 shows the N, P, and K contents as well as the N:P ratio for the roots of *P. australis* at the beginning and end of the experiment for the three sediment types. The N, P, and K contents in the roots increased in time, while the N:P ratio clearly decreased. The reduction in N:P ratio from 11 to 2–3 suggests N was the limiting nutrient as an N:P ratio of < 14 in plant tissue is indicative of N limitation (Koerselman and Meuleman, 1996). However, root N and P concentrations of *P. australis* should typically range between 0.64–1.04% for N and 0.06–0.13% for P (Wang et al., 2015). Figure 4 shows that the root N and P concentrations were above these values, and that P was particularly high: by a factor of 5 to 10 (N: 1.14–1.63% and P: 0.52–0.62%). Hence the concentrations of these nutrients in the roots do not indicate that nutrient limitation is a likely cause of the reduced plant growth and shriveling and yellowing of foliage.

We hypothesize that co-precipitation of P with Fe on roots enhanced the concentrations of P in the plant roots (Snowden and Wheeler, 1995; Jørgenson et al., 2012). Snowden and Wheeler (1995) showed that this so-called iron plaque formation enhances uptake of Fe and P. This may cause iron toxicity and is probably responsible for the elevated P concentrations in tissue, and for the stunted growth and leaf decay we observed in the experiment. Note that the plant roots of *P. australis* initiate this process by oxidizing their environment and thereby enabling ferrous iron to oxidize into P-bearing ferric iron, which precipitates on roots.

The Fe concentration in the leaves and in the roots supports the "Fe-P co-precipitation hypothesis": we measured an approximately 20-fold increase by comparison with the initial concentration in the seedlings (Figure 5). Furthermore, ferric oxide, a product of pyrite oxidation, precipitates on root surfaces (Jørgenson et al., 2012), and hence pyrite oxidation in sediments is directly linked to iron toxicity in plants.

Further evidence to support our hypothesis is provided by the results of the sequential phosphorus extraction conducted on the sediments: it revealed that the dominant P pool in the sediments is the Fe-P fraction (Table 2). P co-precipitates with Fe on roots if it is bound to ferric oxides.

3.5. Implications for eco-engineering

Our results strongly point in the direction of iron toxicity as a major bottleneck prohibiting healthy development of *P. australis*. Since the candidate material for the construction of the Markermeer wetland has high contents of Fe and Fe-P, we recommend using Fe-tolerant plant species as test species in the new wetland, rather than species optimized for growing in N-limited conditions.

Concomitantly with iron toxicity, a high Fe-P content in soil will trigger P mobilization if that soil is rewetted after having dried out and contains high amounts of SO_4 (Smolders and Roelofs, 1993; Lucassen et al., 2005). In some cases, this can result in elevated levels of sulfide, thereby promoting S toxicity in plants (Lamers et al., 1998; Van der Welle et al., 2007).

Figure 6 summarizes the important feedbacks and processes we expect play an important role in the clay-rich sediments. Following the feedback loops between plant and soil, we see a negative feedback loop that arises because plant roots induce aeration, which promotes iron toxicity that decreases plant growth and results in plant death. Also, we see a positive feedback loop, as iron toxicity induces reduction processes as a result of root death, which leads to P mobilization and hence enhances plant growth and regeneration. Negative feedback loops diminish or buffer changes, whereas a positive feedback loop amplifies changes. So, a negative feedback loop normally stabilizes the system, in our case via the toxic effect of iron oxides on plants, but plant growth may increase due to the positive feedback loop via P mobilization. The relative strengths of these two feedback loops and the sensitivity of species to Fe toxicity determine the ultimate effect on vegetation development in wetlands built from these sediments.

As drying–rewetting cycles are likely to occur in these future wetlands and since the Fe-P concentrations in the situated sediment are high, these feedbacks might be an important factor influencing soil formation and ecosystem development. We therefore recommend studying the ultimate effects of the use of this material on ecosystem development by testing with various plant species and drying–rewetting cycles.

Not all environmental factors that potentially interfere with the processes and feedbacks described in this study could be taken into account with this experimental design (e.g. wave action, wind). Therefore, we recommend to carry out experiments on the wetlands themselves once the crest has stabilized sufficiently.

4. Conclusions

The results of this study show that plants expedite biogeochemical processes by oxidizing and modifying their environment, which in turn affects the growth conditions of the plants. In the mud deposits from Markermeer, the key processes influencing pore water chemistry are pyrite oxidation and associated calcite dissolution. The former is especially likely to be important as it is linked to iron toxicity and P mobilization and thus has the potential to initiate two feedback mechanisms between plant and soil. We found strong indications for a negative feedback loop, where plant-induced iron toxicity is hampering plant growth, and a positive feedback loop, where iron toxicity promotes P mobilization, enhancing plant growth. The strength of these feedbacks and the balance between them will play an important role in regulating eco-engineering conditions for plants.

We found conclusive evidence that the low N:P ratio found in plant tissue was not caused by N limitation, as the ratio suggests, but probably results from enhanced P uptake as a result of co-precipitation with Fe on roots.

The magnitudes of the feedback mechanisms are expected to differ between the sediments used. The soft clay-rich layer has less Fe-P than the underlying clay layer and therefore P mobilization is expected to be less in mud. However, when the mud is mixed with sand, the enhanced aeration due to the change in grain-size composition results in higher oxidation rates, increasing the impact of the positive feedback mechanisms involving P mobilization and iron toxicity.

To study the effects of iron toxicity and P mobilization in greater detail, we recommend further testing with different plant species and drying–rewetting cycles. This is important because we expect these mechanisms to influence soil formation and ecosystem development in the created wetlands.

Acknowledgements

This study was supported with funding from Netherlands Organization for Scientific Research (NWO), project no. 850.13.032 and the companies Boskalis and Van Oord. We would also like to thank Botanical Garden Utrecht for their help, support and advice during the greenhouse experiment. Joy Burrough advised on the English. Last, we would like to thank Ingrid Bauer and an anonymous referee for helpful comments on the manuscript.

References

Bauer, A., Velde, B.D.: Soils: Retention and Movement of Elements at the Interface, in: Geochemistry at the Earth's Surface: Movement of Chemical Elements, Springer-Verlag Berlin Heidelberg, New York, 2014.

Belkhiri, L., Boudoukha, A., Mouni, L., Baouz, T.: Application of multivariate statistical methods and inverse geochemical modeling for characterization of groundwater — A case study: Ain Azel plain (Algeria), Geoderma, 159, 390-398, 2010.

Bengough, A.G., Mullins, C.E.: Mechanical impedance to root growth: a review of experimental techniques and root growth responses, Journal of Soils Science, 41, 341-358, 1990.

Borsje, B.W., Van Wesenbeeck, B.K., Dekker, F., Paalvast, P., Bouma, T.J., Van Katwijk, M., De Vries, M.B.: How ecological engineering can serve in coastal protection, Ecological Engineering, 37, 113-122, 2011.

Bradford, M.A., Keiser, A.D., Davies, C.A., Mersmann, C.A., Strickland, M.S.: Empirical evidence that soil carbon formation from plant inputs is positively related to microbial growth, Biogeochemistry, 113, 271-281, 2013.

Brix, H., Borrell, B.K., Schierup, H.H.: Gas fluxes achieved by in situ convective flow in *Phragmites australis*, Aquatic Botany, 54, 151-163, 1996.

Canavan, R.W., Van Cappellen, P., Zwolsman J.J.G., Van den Berg, G.A., Slomp, C.A.: Geochemistry of trace metals in a fresh water sediment: Field results and diagenetic modeling, Science of the Total Environment, 381, 263–279, 2007.

Carucci, V., Petitta, M., Aravena, R.: Interaction between shallow and deep aquifers in the Tivoli Plain (Central Italy) enhanced by groundwater extraction: A multi-isotope approach and geochemical modeling, Applied Geochemistry, 27, 266-280, 2012.

De Lucas Pardo, M.A., Bakker, M., Van Kessel, T., Cozzoli, F., Winterwerp, J.C.: Erodibility of soft freshwater sediments in Markermeer: the role of bioturbation by meiobenthic fauna, Ocean Dynamics, 63, 1137-1150, 2013.

De Lucas Pardo, M.A.: Effect of biota on fine sediment transport processes. A study of lake Markermeer, Ph.D thesis, Delft University, the Netherlands, 211 pp., 2014.

Dickopp, J., Kazda, M., Cízková, H.: Differences in rhizome aeration of *Phragmites australis* in a constructed wetland, Ecological Engineering, 37, 1647-1653, 2011.

Ehrenfeld, J.G., Ravit, B., Elgersma, K.: Feedback in the plant-soil system, Annual Review of Environment and Resources, 30, 75-115, 2005.

Ericsson, T.: Growth and shoot:root ratio of seedlings in relation to nutrient availability, Plant and Soil, 168, 205-214, 1995.

Gerke, J., Beissner, L., Römer W.: The quantitative effect of chemical phosphate mobilization by carboxylate anions on P uptake by a single root. I. The basic concept and determination of soil parameters, Journal of Plant Nutrition and Soil Science, 163, 207-212, 2000.

Holtkamp, R., Van der Wal, A., Kardol, P., Van Putten, W.H., De Ruiter, P.C., Dekker, S.C.: Modelling C and N mineralisation in soil food webs during secondary succession on ex-arable land, Soil Biology and Biochemistry, 43, 251-260, 2011.

Howard, P.J.A.: The Carbon-Organic Matter Factor in Various Soil Types, Oikos, 15, 229-236, 1965.

Jilbert, T., Slomp C.P.: Iron and manganese shuttles control the formation of authigenic phosphorus minerals in the euxinic basins of the Baltic Sea, Geochimica et Cosmochimica Acta, 107, 155–169, 2013.

Jones, C.G., Lawton, J.H., Shachak, M.: Organisms as Ecosystem Engineers, Oikos, 69, 373-386, 1994.

Jørgenson, K.D., Lee, P.F., Kanavillil, N.: Ecological relationships of wild rice, *Zizania* spp. 11. Electron microscopy study of iron plaques on the roots of northern wild rice (*Zizania palustris*), Botany, 91, 189–201, 2012.

Koerselman, W., Meuleman, A.F.M.: The vegetation N:P ratio: a new tool to detect the nature of nutrient limitation, Journal of Applied Ecology, 33, 1441-1450, 1996.

Lambers, H., Mougel, C., Jaillard, B., Hinsinger P.: Plant-microbe-soil interactions in the rhizosphere: an evolutionary perspective, Plant and Soil, 321, 83-115, 2009.

Lamers, L.P.M., Tomassen, H.B.M., Roelofs J.G.M.: Sulfate-Induced Eutrophication and Phytotoxicity in Freshwater Wetlands, Environmental Science and Technology, 32, 199-205, 1998.

Lecomte, K.L., Pasquini, A.I., Depetris, P.J.: Mineral weathering in a Semiarid Mountain River: Its assessment through PHREEQC inverse modeling, Aquatic Geochemistry, 11, 173-194, 2005.

LMRe (Landelijk Meetnet Regenwater): http://www.lml.rivm.nl/gevalideerd/, last access: 17 November 2014, 2014.

Lucassen, E.C.H.E.T., Smolders, A.J.P., Lamers, L.P.M., Roelofs, J.G.M.: Water table fluctuations and groundwater supply are important in preventing phosphate-eutrophication in sulphate-rich fens: Consequences for wetland restoration, Plant and Soil, 269, 109-115, 2005.

Nicholson, R.V., Gillham, R.W., Reardon E.J.: Pyrite oxidation in carbonate-buffered solution: 2. Rate control by oxide coatings, Geochimica et Cosmochimica Acta, 54, 395-402, 1990.

Noordhuis, R., Groot, S., Dionisio Pires, M., Maarse M.: Wetenschappelijk eindadvies ANT-IJsselmeergebied. Vijf jaar studie naar kansen voor het ecosysteem van het IJsselmeer, Markermeer en IJmeer met het oog op de Natura-2000 doelen, Open File Rep. 1207767-000, 98 pp., 2014.

Olde Venterink, H.: Does phosphorus limitation promote species-rich plant communities?, Plant and Soil, 345, 1-9, 2011.

O'Kelly, B.C.: Compression and consolidation anisotropy of some soft soils, Geotechnical and Geological Engineering, 24, 1715-1728, 2006.

Onipchenko, V.G., Makarov, M.I., Van der Maarel, E.: Influence of alpine plants on soil nutrient concentrations in a monoculture experiment, Folia Geobotanica, 36, 225-241, 2001.

Parkhurst, D.L., Appelo, C.A.J.: Description of input and examples for PHREEQC version 3-A computer program for speciation, batch-reaction, one-dimensional transport, and inverse geochemical calculations, U.S. Geological Survey, Denver, 497 pp., 2013.

Prisciandaro, M., Santucci, A., Lancia, A., Musmarra, D.: Role of citric acid in delaying gypsum precipitation, The Canadian journal of Chemical Engineering, 83, 586-592, 2005.

Ruttenberg, K.C.: Development of a sequential extraction method for different forms of phosphorus in marine sediments, Limnology Oceanography, 37, 1460-1482, 1992.

Shipley, B., Meziane D.: The balanced-growth hypothesis and the allometry of leaf and root biomass allocation, Functional Ecology, 16, 326-331, 2002.

Smith, K.E., Luna, T.O.: Radial Oxygen Loss in Wetland Plants: Potential Impacts on Remediation of Contaminated Sediments, Journal of Environmental Engineering, 139, 496-501, 2013.

Smolders, A., Roelofs J.G.M.: Sulphate-mediated iron limitation and eutrophication in aquatic ecosystems, Aquatic Botany, 46, 247-253, 1993.

Snowden, R.E.D., Wheeler, B.D.: Chemical changes in selected wetland plant species with increasing Fe supply, with specific reference to root precipitates and Fe tolerance, New Phytologist, 131, 503-520, 1995.

Taylor, L.L., Leake, J.R., Quirk, J., Hardy, K., Banwart, S.A., Beerling, D.J.: Biological weathering and the long-term carbon cycle: integrating mycorrhizal evolution and function into the current paradigm, Geobiology, 7, 171-191, 2009.

Temmerman, S., Meire, P., Bouma, T.J., Herman, P.M.J., Ysebaert, T., De Vriend, H.K.: Ecosystem-based coastal defence in the face of global change, Nature, 504, 79-83, 2013.

Van der Welle, M.E.W., Smolders, A.J.P., Op den Camp, H.J.P., Roelofs, J.G.M., Lamers, L.P.M.: Biogeochemical interactions between iron and sulphate in freshwater wetlands and their implications for interspecific competition between aquatic macrophytes, Freshwater Biology, 52, 434-447, 2007.

Van Hees, P.A.W., Jones, D.L., Finlay, R., Godbold, D.L., Lundström U.S.: The carbon we do not see—the impact of low molecular weight compounds on carbon dynamics and respiration in forest soils: a review, Soil Biology and Biochemistry, 37, 1-13, 2005.

Van Kessel, T., De Boer, G., Boderie P.: Calibration suspended sediment model Markermeer, Open File Rep. 4612, 107 pp., 2008.

Vijverberg, T., Winterwerp, J.C., Aarninkhof, S.G.J., Drost, H.: Fine sediment dynamics in a shallow lake and implication for design of hydraulic works, Ocean Dynamics, 61, 187-202, 2011.

Voorhees, W.B., Farrel, D.A., Larson, W.E.: Soil strength and aeration effects on root elongation, Soil Science Society of America Journal, 39, 948-953, 1975.

Wang, W.Q., Sardans, J., Wang, C., Zeng, C.S., Tong, C., Asensio, D., Penuelas, J.: Ecological stoichiometry of C, N, and P of invasive Phragmites australis and native Cyperus malaccensis species in the Minjiang River tidal estuarine wetlands of China, Plant Ecology, 216, 809-822, 2015.

Table 1. List of steps used in the extraction procedure of phosphorus (based on Ruttenberg, 1992).

Step		**Extractant**	**Separated P fraction**
I		1M $MgCl_2$, 30 min	Exchangeable or loosely sorbed P
II	A	Citrate-dithionite-bicarbonate (CDB), 8 h	Easily reducible or reactive ferric Fe- P
	B	1M $MgCl_2$, 30 min	
III	A	Na acetate buffer (pH 4), 6 h	Amorphous apatite and carbonate P
	B	1M $MgCl_2$, 30 min	
IV		1M HCl, 24 h	Crystalline apatite and other inorganic P
V		Ash at 550 ^{o}C, 2h; 1M HCl, 24 h	Organic P

Table 2. Geochemical and mineralogical composition of the sediment types used in this study. Significant differences between Mud_{soft} and Clay are indicated by * ($p < 0.05$).

	Unit	n per type	Clay Mean	SD	Mud_{soft} Mean	SD	Mud_{sand} Mean	SD
Aqua regia / CS								
Al*	mg/kg	15	21989	*4512*	16593	*3130*	6394	*2439*
Ca	mg/kg	15	48031	*3032*	45635	*6020*	18877	*3572*
Fe*	mg/kg	15	27766	*3764*	20745	*2987*	7804	*2281*
K	mg/kg	15	5371	*1262*	4102	*641*	1723	*742*
Mg*	mg/kg	15	8041	*1017*	6636	*906*	2531	*558*
Mn*	mg/kg	15	710	*166*	577	*160*	238	*62*
Na*	mg/kg	15	992	*379*	526	*158*	219	*64*
P*	mg/kg	15	1186	*217*	649	*169*	259	*56*
S	mg/kg	15	5727	*710*	5586	*698*	3001	*846*
Sr	mg/kg	15	148	*21*	135	*26*	62	*14*
Ti	mg/kg	15	312	*74*	312	*77*	125	*44*
Zn*	mg/kg	15	159	*58*	110	*29*	43	*18*
Seq. P extraction								
Exchangeable P	mg/kg	15	14.3	*6.81*	11.9	*3.50*	5.9	*1.79*
Fe- bound P*	mg/kg	15	772	*263*	279	*61.7*	94.5	*29.0*
Ca-bound P	mg/kg	15	146	*43.3*	121	*30.9*	36.8	*13.1*
Detrital P	mg/kg	15	147	*16.5*	169	*14.1*	51.5	*10.9*
Organic P	mg/kg	15	99.6	*20.0*	117	*25.1*	47.7	*8.38*
XRD								
Quartz	%	1	48		37		n.a.	
Calcite	%	1	9		9		n.a.	
Pyrite	%	1	0.6		0.6		n.a.	
Illite	%	1	15		21		n.a.	
Smectite	%	1	11		14		n.a.	
Kaolinite	%	1	3		5		n.a.	
Chlorite	%	1	2		3		n.a.	
Other								
Organic matter	%	5	6.7	*0.6*	7.2	*0.6*	2.8	*0.4*
CEC (calculated)	meq/100g		30.0		37.2		12.4	

Table 3. Main pore water processes expressed in mole transfers (µmol l^{-1} day^{-1}) as modeled by PHREEQC with pore water data retrieved at 1 cm and 11 cm below sediment surface (D_1 and D_{11} respectively). Positive values indicate dissolution, negative values indicate precipitation. Cation exchange capacity (CEC) is the sum of Ca, Fe, K, Mg, Na, and NH_4.

			Calcite		Gypsum		$Fe(OH)_3$		Pyrite		ΣCEC		H_2O (x 10^3)		O_2	
Phase	**Condition**		D_1	D_{11}	D_1	D_{11}	D_1	D_{11}	D_1	D_{11}	D_1	D_{11}	D_1	D_{11}	D_1	D_{11}
1. Oxidation t=0-22 days	**Mud_{soft}**	**No plant**	267	111	*0.00*	-72.5	-277	*0.00*	270	36.2	-31.3	20.2	-3364	*0.00*	1009	119
	Mud_{sand}	**No plant**	*0.00*	59.6	*0.00*	-40.7	-116	*0.00*	109	21.7	-4.99	7.92	-2591	*0.00*	432	69.5
	Clay	**No plant**	120	55.2	*0.00*	-53.4	-160	*0.00*	159	20.1	-91.4	14.0	-2364	*0.00*	659	61.9
2. Initial root development t=22-64 days	**Mud_{soft}**	**No plant**	27.1	*0.00*	-236	*0.00*	0.95	-0.24	*0.00*	*0.00*	-23.1	1.43	*0.00*	*0.00*	2.62	*0.00*
		Plant	48.8	19.8	-208	-3.81	-10.0	-6.19	9.76	*0.00*	-7.63	1.43	*0.00*	*0.00*	45.5	*0.00*
	Mud_{sand}	**No plant**	39.3	71.7	*0.00*	*0.00*	*0.00*	-41.2	0.21	*0.00*	1.90	1.46	380	*0.00*	*0.00*	*0.00*
		Plant	7.10	83.8	-83.4	*0.00*	*0.00*	-51.2	3.58	*0.00*	5.40	3.40	-996	*0.00*	*0.00*	*0.00*
	Clay	**No plant**	*0.00*	27.1	-32.1	*0.00*	-21.4	-25.0	21.2	*0.00*	0.01	-0.23	-286	*0.00*	41.9	*0.00*
		Plant	36.9	16.2	*0.00*	*0.00*	-14.3	*0.00*	64.3	11.9	28.4	4.53	-6.67	*0.00*	186	40.5
3. Root influence t=64-176 days	**Mud_{soft}**	**No plant**	*0.00*	-3.21	-19.2	*0.00*	-1.34	-0.80	*0.00*	*0.00*	-1.07	-1.43	56.3	*0.00*	*0.00*	*0.00*
		Plant	25.8	*0.00*	*0.00*	*0.00*	-4.20	*0.00*	23.8	4.11	7.88	-4.65	49.1	*0.00*	83.6	13.6
	Mud_{sand}	**No plant**	8.13	*0.00*	-7.59	*0.00*	-10.6	-1.34	*0.00*	*0.00*	-1.78	1.42	74.1	*0.00*	*0.00*	*0.00*
		Plant	*0.00*	*0.00*	-14.8	*0.00*	-13.3	-23.2	13.8	7.95	0.12	-10.6	-357	-652	44.7	32.6
	Clay	**No plant**	*0.00*	11.5	*0.00*	*0.00*	*0.00*	-13.8	33.3	*0.00*	23.9	0.36	134	*0.00*	113	*0.00*
		Plant	115	18.7	*0.00*	*0.00*	-58.5	-8.48	58.3	8.57	45.4	-5.73	*0.00*	-98.2	215	28.4

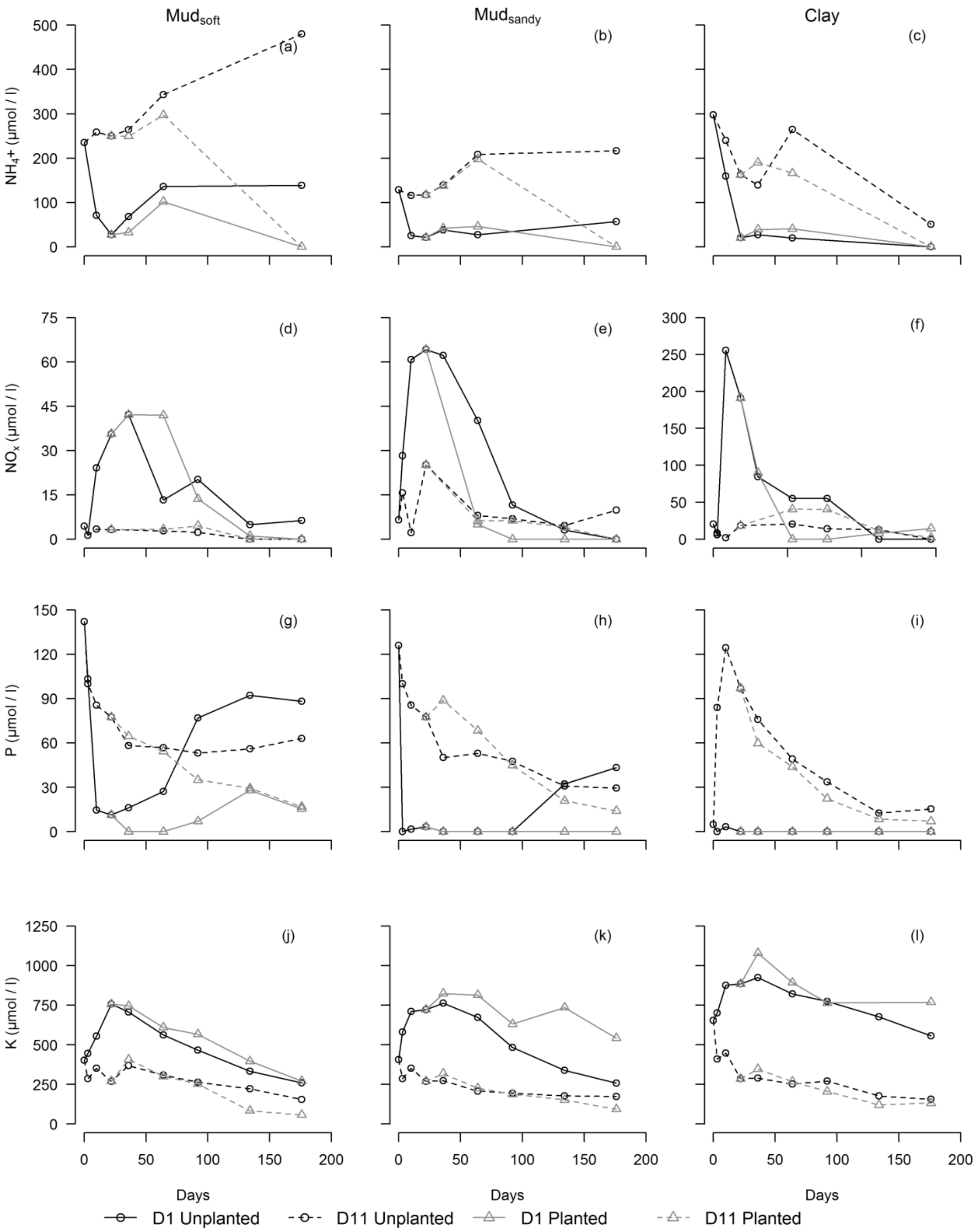

Figure 1. Time series of NH_4 (a–c), NO_x (d–f), P (g–i) and K (j–l) concentrations. Each column represents one sediment type: Mud$_{soft}$ (a, d, g, j), Mud$_{sand}$ (b, e, h, k), and Clay (c, f, i, l). The variable and the scale of the x-axis are the same for each row, except for the scale in f.

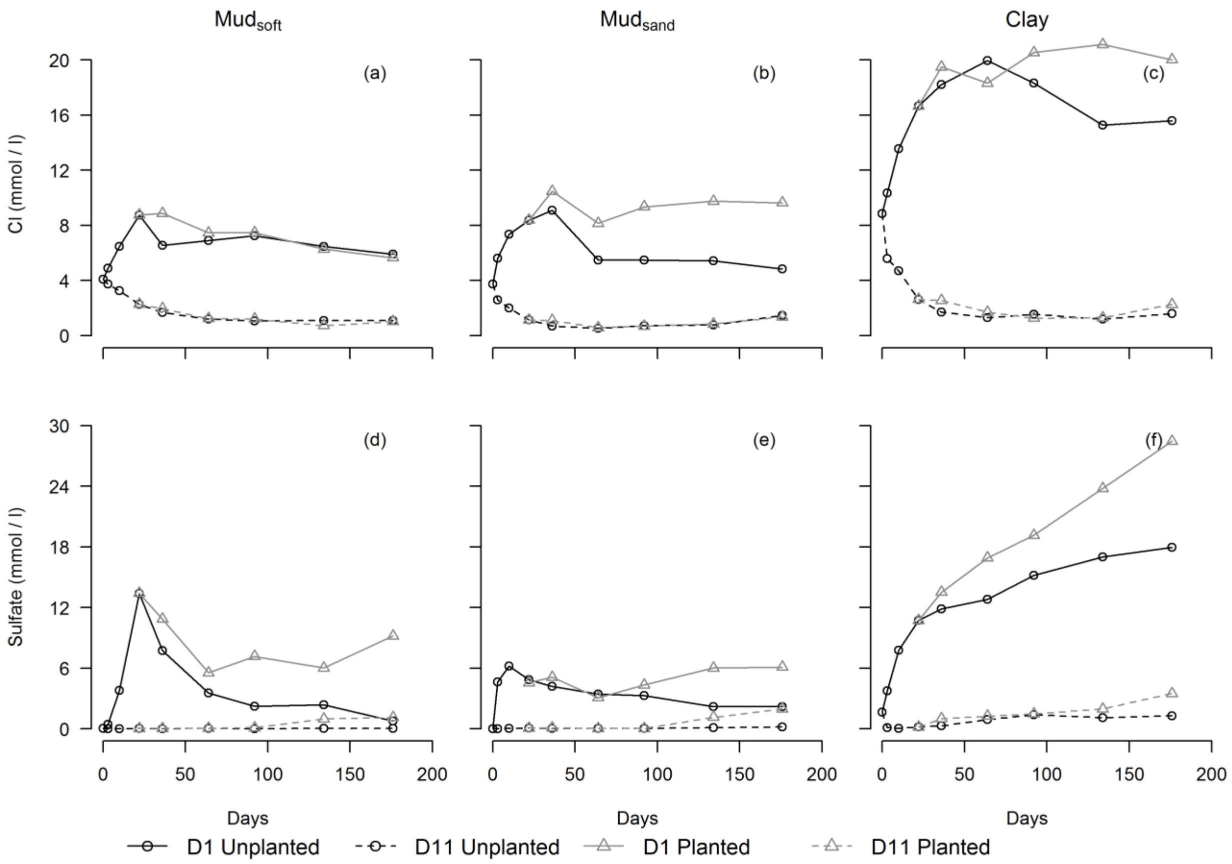

Figure 2. Time series of Cl (a–c) and sulfate (d–f) concentrations. Each column represents one sediment type: Mud_{soft} (a, d), Mud_{sand} (b, e), and Clay (c, f). The variable and the scale of the x-axis are the same for each row.

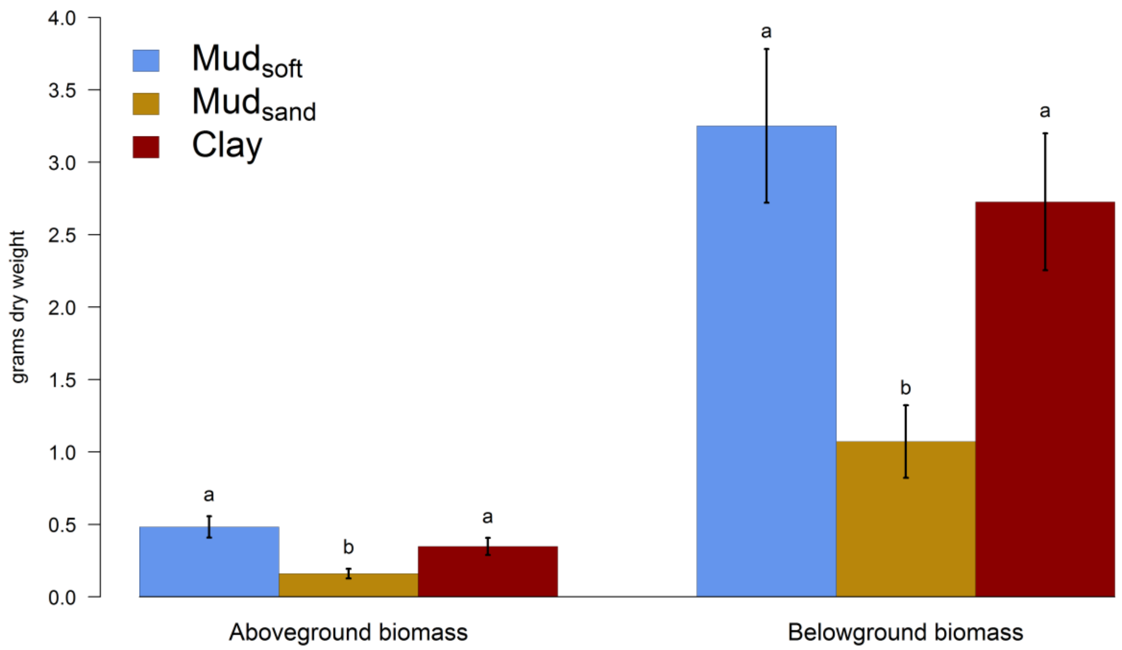

Figure 3. Above- and belowground biomass in grams dry weight, with error bars (n = 5). Significant differences between sediment types are indicated by different letters, and non-significant differences are indicated by a similar letter.

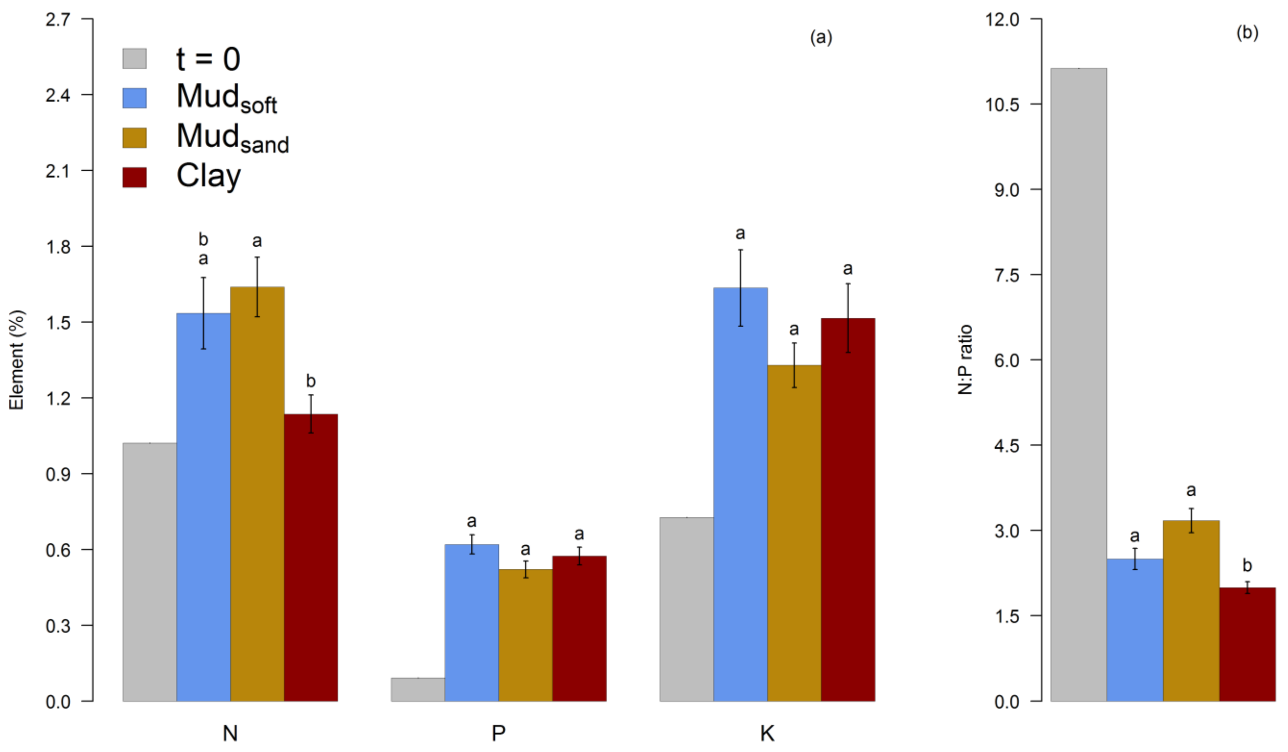

Figure 4. N, P, and K concentration in root tissue (t = 176) in % of dry weight (a) as well as the N:P ratio (b) with error bars when n = 5. Significant differences between sediment types are indicated by different letters, and non-significant differences are indicated by a similar letter.

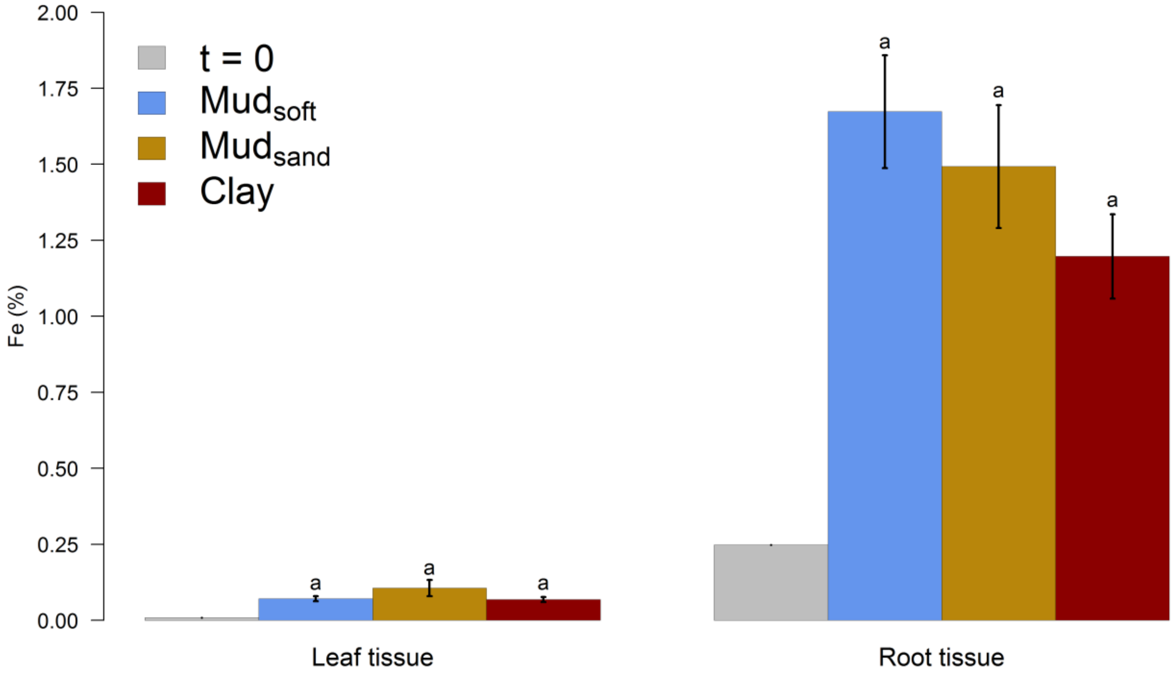

Figure 5. Fe concentration (% of dry weight) in leaf and root tissue with error bars when n = 5. Significant differences between sediment types are indicated by different letters, and non-significant differences are indicated by a similar letter.

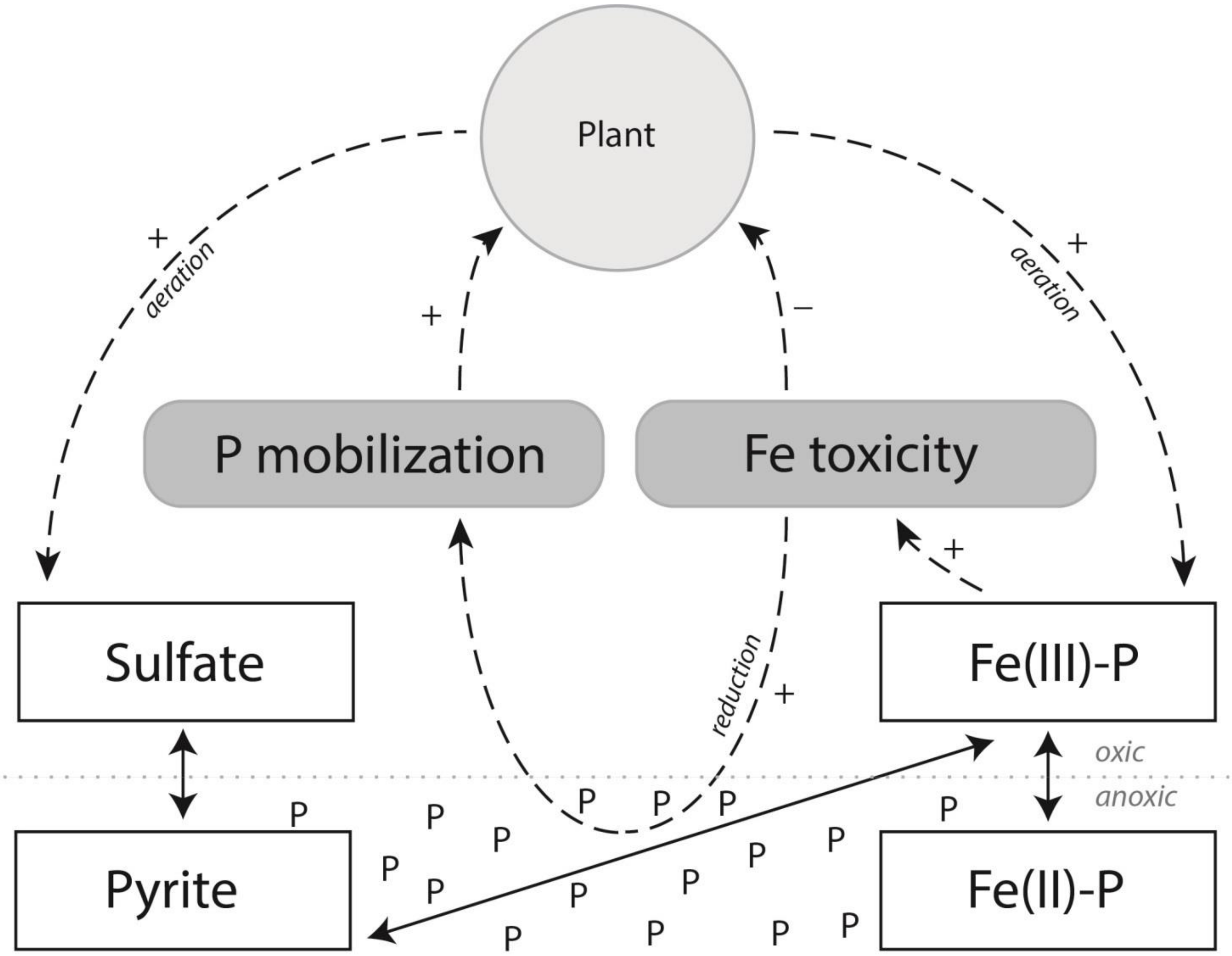

Figure 6. Most important biogeochemical processes and feedbacks identified in this study. + indicates positive feedback, - indicates negative feedback.

Appendix

Table A1. Pore water processes expressed in mole transfers (μmol l^{-1} day^{-1}) as modeled by PHREEQC with pore water data retrieved at 1 cm below sediment surface. Positive values indicate dissolution, negative values indicate precipitation.

		Phase 1. Oxidation (t=0-22)			Phase 2. Initial root development (t=22-64)						Phase 3. Root influence (t=64-176)					
		No plant	No plant	No plant	No plant	Plant	No plant	Plant	No plant	Plant	No plant	Plant	No plant	Plant	No plant	Plant
Reactant	**Composition**	**Mud_{soft}**	**Mud_{sand}**	**Clay**	**Mud_{soft}**		**Mud_{sand}**		**Clay**		**Mud_{soft}**		**Mud_{sand}**		**Clay**	
Calcite	**$CaCO_3$**	267	*0.00*	120	27.1	48.8	39.3	7.1	*0.00*	36.9	*0.00*	25.8	8.13	*0.00*	*0.00*	115
Gypsum	**$CaSO_4$:$2H_2O$**	*0.00*	*0.00*	*0.00*	-236	-208	*0.00*	-83.4	-32.1	*0.00*	-19.2	*0.00*	-7.59	-14.8	*0.00*	*0.00*
Hydroxyapatite	**$Ca_5(PO_4)_3(OH)$**	-5.00	-3.64	*0.00*	0.24	*0.00*	-0.02	-0.04	*0.00*	*0.00*	0.18	*0.00*	0.09	*0.00*	*0.00*	*0.00*
Chalcedony	**SiO_2**	-19.1	-15.5	-18.2	0.95	0.71	1.91	-3.37	-1.67	-2.14	0.71	*0.00*	0.54	1.43	*0.00*	-0.36
$Fe(OH)_3$ (a)	**$Fe(OH)_3$**	-277	-116	-160	0.95	-10.0	*0.00*	*0.00*	-21.4	-14.3	-1.34	-4.20	-10.6	-13.3	*0.00*	-58.5
Pyrite	**FeS_2**	270	109	159	*0.00*	9.76	0.21	3.58	21.2	64.3	0.00	23.8	0.00	13.8	33.3	58.3
Rhodochrosite	**$MnCO_3$**	-11.8	-11.4	-2.27	2.86	1.19	1.23	0.34	-0.24	-0.24	-0.63	-0.89	0.09	0.18	*0.00*	*0.00*
CEC	**CaX_2**	*0.00*	20.9	55.5	63.1	41.9	-9.11	*0.00*	*0.00*	*0.00*	2.50	*0.00*	-9.73	*0.00*	-9.64	-85.4
	FeX_2	*0.00*	*0.00*	*0.00*	*0.00*	*0.00*	-0.19	-4.11	*0.00*	-50.2	1.61	-19.8	11.7	*0.00*	-33.3	*0.00*
	KX	-8.64	-5.00	-17.7	-4.76	*0.00*	3.78	-8.30	-6.19	*0.00*	-2.14	-2.14	-2.77	-7.68	*0.00*	*0.00*
	MgX_2	31.4	-16.8	36.8	-39.8	-30.5	7.42	-1.35	*0.00*	21.7	-3.04	12.0	*0.00*	*0.00*	19.1	39.8
	NaX	-20.9	*0.00*	-166	-46.4	-25.7	*0.00*	25.1	25.2	77.6	*0.00*	19.7	*0.00*	12.0	49.4	92.9
	NH_4X	-33.2	-4.09	*0.00*	4.76	6.67	*0.00*	-5.94	-19.0	-20.7	*0.00*	-1.88	-0.98	-4.20	-1.70	-1.88
H_2O (g)	**$H_2O \times 10^3$**	-3364	-2591	-2364	*0.00*	*0.00*	380	-996	-286	-6.67	56.3	49.1	74.1	-357	134	*0.00*
O_2 (g)	**O_2**	1009	432	659	2.62	45.5	*0.00*	*0.00*	41.9	186	*0.00*	83.6	*0.00*	44.7	113	215
CO_2 (g)	**CO_2**	-827	-532	-650	35.2	*0.00*	39.7	*0.00*	-55.5	-84.8	*0.00*	-33.1	*0.00*	44.6	-31.7	-115
	No. models found	2	2	2	3	4	2	2	5	2	6	2	1	2	2	1

Table A2. Pore water processes expressed in mole transfers (µmol l^{-1} day^{-1}) as modeled by PHREEQC with pore water data retrieved at 11 cm below sediment surface. Positive values indicate dissolution, negative values indicate precipitation.

		Phase 1. Oxidation (t=0-22)			Phase 2. Initial root development (t=22-64)						Phase 3. Root influence (t=64-176)					
		No plant	No plant	No plant	No plant	Plant	No plant	Plant	No plant	Plant	No plant	Plant	No plant	Plant	No plant	Plant
Reactant	**Composition**	Mud_{soft}	Mud_{sand}	Clay	Mud_{soft}		Mud_{sand}		Clay		Mud_{soft}		Mud_{sand}		Clay	
Calcite	**$CaCO_3$**	111	59.6	55.2	0.00	19.8	71.7	83.8	27.1	16.2	-3.21	0.00	0.00	0.00	11.5	18.7
Gypsum	**$CaSO_4$:$2H_2O$**	-72.5	-40.7	-53.4	0.00	-3.81	0.00	0.00	0.00	0.00	0.00	0.00	0.00	0.00	0.00	0.00
Hydroxyapatite	**$Ca_5(PO_4)_3(OH)$**	0.00	0.51	1.45	-0.24	0.00	0.00	0.00	0.00	0.00	0.00	-0.09	0.00	-0.45	0.00	-0.18
Chalcedony	**SiO_2**	4.44	5.32	6.74	1.90	3.33	3.10	3.81	1.67	0.95	-0.18	-1.07	-0.27	-3.48	0.00	-1.07
$Fe(OH)_3$ (a)	**$Fe(OH)_3$**	0.00	0.00	0.00	-0.24	-6.19	-41.2	-51.2	-25.0	0.00	-0.80	0.00	-1.34	-23.2	-13.8	-8.48
Pyrite	**FeS_2**	36.2	21.7	20.1	0.00	0.00	0.00	0.00	0.00	11.9	0.00	4.11	0.00	7.95	0.00	8.57
Rhodochrosite	**$MnCO_3$**	0.00	1.18	0.31	0.00	0.48	1.19	0.95	0.00	0.24	0.00	0.00	0.00	-0.71	0.18	0.09
CEC	**CaX_2**	0.00	0.00	0.00	-1.43	-5.95	-50.7	-63.3	-7.86	0.00	1.70	8.39	0.00	0.00	-3.75	0.00
	FeX_2	-35.5	-20.9	-19.0	0.00	0.00	42.4	51.7	0.00	-11.9	1.07	-3.66	-0.54	15.2	4.29	0.00
	KX	7.00	5.87	3.76	0.00	0.00	2.62	2.86	-5.95	1.67	-0.89	-1.79	0.00	-3.84	0.00	-1.70
	MgX_2	15.4	13.0	4.87	0.00	4.76	7.14	8.57	8.10	7.38	-1.25	0.00	0.00	-4.11	2.59	5.71
	NaX	25.2	9.95	24.4	0.00	0.00	0.00	5.24	0.00	6.43	-4.29	-4.20	1.96	-12.4	0.00	-5.54
	NH_4X	8.12	0.00	0.00	2.86	2.62	0.00	-1.67	5.48	0.95	2.23	-3.39	0.00	-5.80	-2.77	-4.20
H_2O (g)	**H_2O x 10^3**	0.00	0.00	0.00	0.00	0.00	0.00	0.00	0.00	0.00	0.00	0.00	0.00	-652	0.00	-98.2
O_2 (g)	**O_2**	119	69.5	61.9	0.00	0.00	0.00	0.00	0.00	40.5	0.00	13.6	0.00	32.6	0.00	28.4
CO_2 (g)	**CO_2**	156	0.00	43.0	0.00	0.00	0.00	0.00	0.00	14.5	0.00	0.00	0.00	-67.3	0.00	-13.7
	No. models found	2	2	1	4	4	2	2	3	2	1	4	2	4	2	1